Article

Valorization of *Agave angustifolia* Bagasse Biomass from the Bacanora Industry in Sonora, Mexico as a Biochar Material: Preparation, Characterization, and Potential Application in Ibuprofen Removal

Hylse Aurora Ruiz-Velducea [1,2], María de Jesús Moreno-Vásquez [2,*], Héctor Guzmán [1,*], Javier Esquer [1], Francisco Rodríguez-Félix [3], Abril Zoraida Graciano-Verdugo [2], Irela Santos-Sauceda [4], Idania Emedith Quintero-Reyes [5], Carlos Gregorio Barreras-Urbina [6], Claudia Vásquez-López [7], Silvia Elena Burruel-Ibarra [4], Karla Hazel Ozuna-Valencia [3] and José Agustín Tapia-Hernández [3,*]

[1] Programa de Posgrado en Sustentabilidad, Departamento de Ingeniería Industrial (DII), Universidad de Sonora, Blvd. Luis Encinas y Rosales, S/N, Colonia Centro, Hermosillo 83000, Sonora, Mexico; a221230205@unison.mx (H.A.R.-V.); javier.esquer@unison.mx (J.E.)

[2] Departamento de Ciencias Químico-Biológicas (DCQB), Universidad de Sonora, Blvd. Luis Encinas y Rosales, S/N, Colonia Centro, Hermosillo 83000, Sonora, Mexico; abril.graciano@unison.mx

[3] Departamento de Investigación y Posgrado en Alimentos (DIPA), Universidad de Sonora, Blvd. Luis Encinas y Rosales, S/N, Colonia Centro, Hermosillo 83000, Sonora, Mexico; francisco.rodriguezfelix@unison.mx (F.R.-F.); a215208659@unison.mx (K.H.O.-V.)

[4] Departamento de Investigación en Polímeros y Materiales (DIPM), Universidad de Sonora, Blvd. Luis Encinas y Rosales, S/N, Colonia Centro, Hermosillo 83000, Sonora, Mexico; irela.santos@unison.mx (I.S.-S.); silvia.burruel@unison.mx (S.E.B.-I.)

[5] Departamento de Ciencias de la Salud (DCS), Universidad de Sonora, Campus Cajeme, Blvd. Bordo Nuevo N/N, Antiguo Ejido Providencia, Ciudad Obregón 85010, Sonora, Mexico; idania.quintero@unison.mx

[6] Centro de Investigación en Alimentación y Desarrollo (CIAD), A. C., Coordinación de Tecnología de Alimentos de Origen Vegetal, Carretera Gustavo Enrique Astiazarán Rosas, Núm. 46, La Victoria, Hermosillo C.P. 83304, Sonora, Mexico; carlosgbarrerasu@gmail.com

[7] Centro de Investigación Científica de Yucatán (CICY), Calle 43 # 130 x 32 y 34, Colonia Chuburná de Hidalgo, Mérida C.P. 97205, Yucatán, Mexico; claudia.vasquez@iq.uson.mx

* Correspondence: mariadejesus.moreno@unison.mx (M.d.J.M.-V.); hector.guzman@unison.mx (H.G.); joseagustin.tapia@unison.mx (J.A.T.-H.)

Abstract: The aim of this research was to separate the over-the-counter nonsteroidal anti-inflammatory drug (NSAID), ibuprofen, from an aqueous solution using the adsorption method, as this NSAID is one of the most globally consumed. An adsorbent was crafted from the *Agave angustifolia* bagasse, a byproduct of the bacanora industry (a representative alcoholic beverage of the state of Sonora, in northwestern Mexico). Three bioadsorbents (BCT1, BCT2, and BCT3) were produced via pyrolysis at a temperature of 550 °C, with slight variations in each process for every bioadsorbent. The bioadsorbents achieved material yields of 25.65%, 31.20%, and 38.28% on dry basis respectively. Characterization of the bagasse and adsorbents involved scanning electron microscopy (SEM), Fourier-transform infrared spectroscopy (FT-IR), thermogravimetric analysis (TGA), and differential scanning calorimetry (DSC). The biomass morphology exhibited a cracked surface with holes induced via the bacanora production process, while the surface of the bioadsorbents before ibuprofen adsorption was highly porous, with a substantial surface area. After adsorption, the surface of the bioadsorbents was transformed into a smoother grayish layer. The macromolecules of cellulose, hemicellulose, and lignin were present in the biomass. According to functional groups, cellulose and hemicellulose degraded to form the resulting bioadsorbents, although traces of lignin persisted after the pyrolysis process was applied to the biomass. In an adsorption study, BCT1 and BCT2 bioadsorbents successfully removed 100% of ibuprofen from aqueous solutions with an initial concentration of 62.6 mg/L. In conclusion, the biocarbon derived from *Agave angustifolia* bagasse exhibited significant potential for removing ibuprofen via adsorption from aqueous solutions.

1. Introduction

Emerging contaminants, defined as substances that were not previously identified or recognized as pollutants, have become a significant interest in science due to growing concern about the potential consequences of their occurrence, although their presence in the natural environment is not a recent phenomenon [1]. These substances have been sporadically detected in the environment, including in water sources, groundwater, and even drinking water [2]. Pharmaceuticals, such as anti-inflammatories, antibiotics, antivirals, and analgesics, represent examples of these emerging contaminants [3,4]. The European Union, the United States, and China have regulatory frameworks for monitoring such contaminants. However, in many countries, they are not regulated by any law or authority [5,6].

In recent decades, ibuprofen has become one of the most widely consumed over-the-counter nonsteroidal anti-inflammatory drugs (NSAIDs) [7]. Its physicochemical properties contribute to high mobility in aquatic environments, making it a significant contaminant in aquatic ecosystems [8]. Studies have indicated that its environmental presence poses a risk of long-term exposure and chronic toxic effects on organisms [9–11]. Ibuprofen can enter aquatic environments through various pathways originating from anthropogenic activities. Improper disposal, including flushing unused medications down the drain, contributes significantly. Manufacturing plants and wastewater treatment plants (WWTPs) are also sources, as ibuprofen is excreted by humans and animals in its unmetabolized form, along with its more toxic metabolites. Also, ibuprofen wastewater effluents from various sources such as veterinary facilities, domestic premises, hospitals, and drug-production factories; these pose environmental concerns due to their potential impact on aquatic ecosystems. Once in the environment, ibuprofen can travel through rivers, lakes, and oceans, contaminating aquatic ecosystems. It can also seep into soil and groundwater, further spreading its presence. Aquatic plants and organisms inadvertently consume ibuprofen, incorporating it into the food web [12,13].

Various methods exist for removing ibuprofen from aqueous solutions, including ozonation and electro-Fenton oxidation [14–16]. Even though these methods have proven effective, their application involves high costs. Consequently, environmentally friendly and economically viable techniques, such as adsorption, have gained interest [17–19]. The use of natural sorbents, like biochar, facilitates efficient and economically viable adsorption processes due to the nature of the adsorptive materials employed [20]. Biochar, a carbon-rich, porous, aromatic, and stable material produced from biomass carbonization under high-temperature and oxygen-limited conditions, possesses excellent physicochemical properties. Its adjustable surface area, controllable porous structures, and abundant oxygen functional groups make it applicable in different fields, including energy, environment, and agriculture [21]. Biochar, generated primarily from biomass wastes through pyrolysis at temperatures ranging from 500 to 800 °C and durations of 1 to 2 h under an inert atmosphere, serves as a versatile tool for circular waste utilization and sustainability. Its applications extend to environmental remediation, including the removal of water pollutants, amelioration of soil quality, and reduction in solid waste [22]. A highly promising application of biochar lies in its ability to effectively capture and retain various pollutants from water sources and can be used as organic fertilizer as well as soil amendment thanks to its porous structure [23]. For the removal of contaminants, the choice of precursor (biomass) is crucial for economic feasibility and efficiency. The precursor should be readily available, low-cost, nonhazardous, with a high carbon and oxygen content, a resistance to abrasion, high thermal stability, and have small pore diameters [24,25].

The current research focused on elucidating the absorption mechanisms of biocarbons, applying them to various emerging pharmaceuticals, and enhancing their surface proper-

ties. In this regard, different absorption mechanisms were elucidated, such as the biocarbon surface exhibiting flaky structures with numerous small pores, enhancing permeability and porosity and providing ample vacant sites for adsorption. Additionally, identified oxygen-containing molecules on the biocarbon surface facilitating the adsorption of emerging pharmaceuticals through significant hydrogen bonding interactions. Furthermore, the sulfonyl group present in many emerging pharmaceuticals enables π-π electron interactions with the benzene ring, which is particularly evident around neutral pH levels, while electrostatic and coordination interactions further contribute to the adsorption of these pharmaceuticals onto the biocarbon surface [26]. Hence, the ongoing research is centered on the production and application of a novel biocarbon derived from the food industry with high adsorption capacity and with the potential to remove ibuprofen.

The traditional bacanora industry in the state of Sonora, Mexico, benefits the region socially, economically, and culturally. Bacanora, a distilled alcoholic beverage, has been produced in the state for over 300 years, involving the processing and distillation of *Agave angustifolia* [27,28]. Annually, around 1.5 million tons of agave are used for alcoholic beverage production, generating approximately 14.41 tons of bagasse per harvested hectare [29,30]. This waste is considered an environmental problem due to its natural degradation by altering soil pH, causing landscape deterioration, generating odors, attracting rodents, and when burnt, releasing greenhouse gases [31]. Given its components and characteristics, the *Agave angustifolia* bagasse resulting from the bacanora production process is considered a lignocellulosic material. Authors argue that such materials have great potential for the production of biopolymers via cellulolytic bacteria and for obtaining phenolic compounds, due to their low cost and abundance [32]. The use of this waste could contribute to the region's economic growth and mitigate environmental impact by avoiding excessive use of natural resources [33]. In this regard, *Agave angustifolia* has been used for the production of biochar and activated carbon [34,35], however, it has not been tested for the removal of emerging pharmaceuticals such as ibuprofen. Thus, utilizing *Agave angustifolia* bagasse biomass from the bacanora industry in Sonora, Mexico, as biochar material may result in a biochar product with favorable properties for effective adsorption of ibuprofen, thus offering a promising approach for water remediation applications.

Therefore, this project aimed to prevent, eliminate, and/or reduce environmental contamination caused by ibuprofen by removing it from a synthetic aqueous solution. Additionally, it sought to add value to the *Agave angustifolia* bagasse by producing a bioadsorbent. Both the bagasse and the resulting biochar treatments were characterized using scanning electron microscopy (SEM), infrared spectroscopy (FTIR), thermogravimetric analysis (TGA), and differential scanning calorimetry (DSC). The potential application of these materials in ibuprofen removal was also explored.

2. Materials and Methods

2.1. Reagents

Distilled water, infant-type suspended ibuprofen, and hydrochloric acid (HCl) were employed in adsorption tests.

2.2. Biomass Acquisition and Conditioning

The *Agave angustifolia* bagasse was donated by the Agave and Bacanora Producers Association in Hermosillo, Sonora, Mexico, to the University of Sonora. The agave residue underwent a drying and grinding process using the methodology described by Robles-García et al. [36] with some adaptations. The bagasse was shredded using a forage shredder. Subsequently, the resulting product was dried in a tunnel at 80 °C for 2 h to reduce particle size. The dried bagasse fibers were further processed with a Pulvex 200 device after sieving them with a 100-mesh screen. The obtained powder underwent a second sieving process to ensure uniform particle size. Particles that did not pass through the 100-mesh screen were subjected to additional crushing until achieving a consistent particle size (Figure 1).

(A)   (B)

Figure 1. Raw material used for bioadsorbent preparation: (**A**) *Agave angustifolia* bagasse, (**B**) conditioned *Agave angustifolia* bagasse.

2.3. Proximal Analysis of Biomass

Mexican standards NOM-116-SSA1-1994, and NMX-F-607-NORMEX-2020, as well as the ASTM E872 Standard, were employed for calculating the percentage of moisture, ash and, volatile matter respectively [37–39]. Additionally, fixed carbon was obtained via percentage difference using the following formula:

$$\text{Fixed carbon } (\%) = 100 - \%\text{ Moisture} - \%\text{ Ash} - \%\text{ Volatile matter} \qquad (1)$$

2.4. Bioadsorbent Preparation

Bioadsorbents BCT1, BCT2, and BCT3 were prepared (Figure 2). Before subjecting the biomass samples to each treatment, they were dried and weighed. The carbonization processes were carried out using an 18.6 L INDBERG-BLUE M muffle furnace. For bioadsorbent BCT1, four crucibles were placed in the muffle at an initial temperature of 24 °C, each containing 5 g of biomass. Once the temperature reached 550 °C, the equipment was turned off and after a 20 s wait, the samples were left inside for 5 min before being removed and placed in a desiccator. The process was repeated for bioadsorbent BCT2, with the only variation being that the initial muffle temperature was 550 °C, and the bioadsorbent was removed immediately after the 20 s and placed in a desiccator. Finally, for bioadsorbent BCT3, the same procedure as for BCT2 was followed, except that the bioadsorbent was removed after 20 s in the muffle and was reintroduced into the equipment and exposed to 550 °C for an additional 20 s before being removed again and placed in a desiccator.
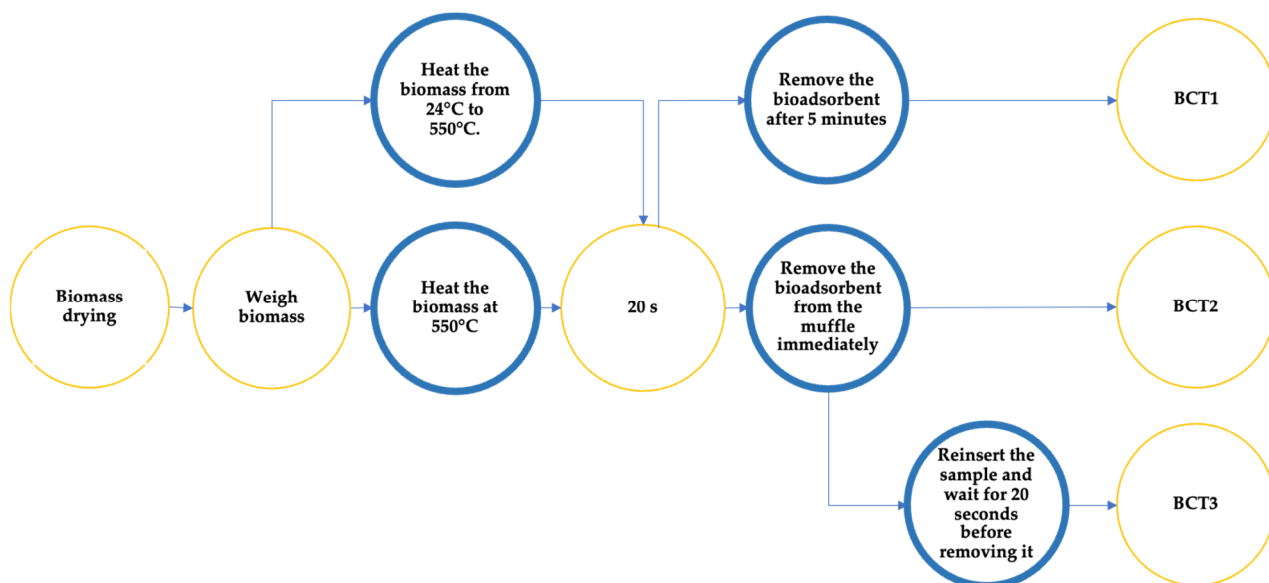
Figure 2. Preparation processes of bioadsorbents BCT1, BCT2, and BCT3.

2.5. Characterization of Agave angustifolia Bagasse and Bioadsorbents

2.5.1. Bioadsorbent Yield

The calculation of the bioadsorbent yield on dry basis was carried out using the following formula:

$$\text{Yield } (\%) = \frac{\text{Weight of obtained bioadsorbent}}{\text{Weight of dry biomass}} \times 100. \qquad (2)$$

2.5.2. Scanning Electron Microscopy (SEM)

Both the biomass and the bioadsorbents underwent morphological characterization using scanning electron microscopy (SEM) with a scanning electron microscope (JEOL JSM-5410LV, Tokyo, Japan). This system operated at an acceleration voltage of 20 kV and a magnification of 10,000×.

2.5.3. Fourier-Transform Infrared Spectroscopy (FTIR)

The identification of different functional groups in biomass and the three bioadsorbents was carried out via Fourier-transform infrared spectroscopy (FTIR) using a PerkinElmer Frontier spectrometer with an attenuated total reflection (ATR) accessory and a transmittance scale ranging from 4000 cm^{-1} to 500 cm^{-1}.

2.6. Thermal Analysis

2.6.1. Thermogravimetric Analysis (TGA)

Thermogravimetric analyses (TGA) and first derivative analyses (DTG) of the starting compounds and resulting bioadsorbents were conducted to study the degradation behavior concerning temperature, ranging from 0 °C to 700 °C. The PerkinElmer TGA-8000 equipment (PerkinElmer, Shelton, CT, USA) was utilized for this purpose.

2.6.2. Differential Scanning Calorimetry (DSC)

The temperature at which specific phase transitions occurred in the bioadsorbents was determined via differential scanning calorimetry (DSC) using a conventional Perkin Elmer DSC model 8500 over a temperature range from 20 °C to 220 °C.

2.7. Preliminary Adsorption Tests

2.7.1. Preparation of Mother Solution

A quantity of 100 mL of mother solution was prepared with a concentration of lignin. The ibuprofen used originated from an infant suspension (Motrin) and was chosen to facilitate dilution in the solution and avoid the use of substances with significant environmental risks. After preparing the solution, pH was measured using a pocket pH/temperature meter, pHep®4, with a resolution of 0.1. The pH was adjusted to 2 by adding drops of hydrochloric acid (HCl). Finally, the adsorption experiments were conducted.

2.7.2. Adsorption Experiments

For the experiment setup, 10 mL of the mother solution was dispensed into a precipitate beaker containing each bioadsorbent. Subsequently, 0.041 g of bioadsorbent was added to each beaker, excluding the control beaker. These containers were covered with Parafilm and placed on plates with a constant stirring speed of 150 rpm for 48 h. At the end of this period, samples were extracted from the beakers and subjected to centrifugation at 6000 gravities at 4 °C for 30 min. Later, the resulting supernatant from each bioadsorbent was analyzed using a UV–visible spectrophotometer, Thermo Scientific Series US 6,414,753 B1 (Thermo Scientific, Waltham, MA, USA) at a maximum adsorption wavelength of 253 nm, which is the wavelength of ibuprofen.

2.7.3. Demonstration of Bioadsorbent Functionality

To exhibit the functionality of the bioadsorbents developed from *Agave angustifolia* bagasse, the samples (bioadsorbent + ibuprofen) were analyzed using scanning electron microscopy (SEM) with the aim of observing crystalline structures and reliefs derived from adsorption in the micrographs. Additionally, the samples were analyzed via Fourier-transform infrared spectroscopy (FTIR) to describe the physical interactions between the bioadsorbent and ibuprofen, thus elucidating a potential adsorption mechanism.

2.8. Statistical Analysis

Proximal analyses were conducted in quadruplicate to determine average values and standard deviations.

3. Results

3.1. Bioadsorbent Preparation

The bioadsorbents from each treatment displayed similar color and texture (Figure 3). The bioadsorbent yield of 25.65% (BTC1), 31.20% (BTC2), and 38.28% (BTC3) were relatively high compared to previous research using lignocellulosic biomass under similar conditions, were yields ranged from 1.27% to 18.48% [40]. Similar findings were reported (25% to 32%) for biomass exposed to 400 °C to 550 °C [41]. These findings align with expectations, as efficient biomass calcination typically yield 30% to 40% [42]. However, as corroborated by various studies, the yield of pyrolyzed sorbents is highly dependent on the raw material [43].
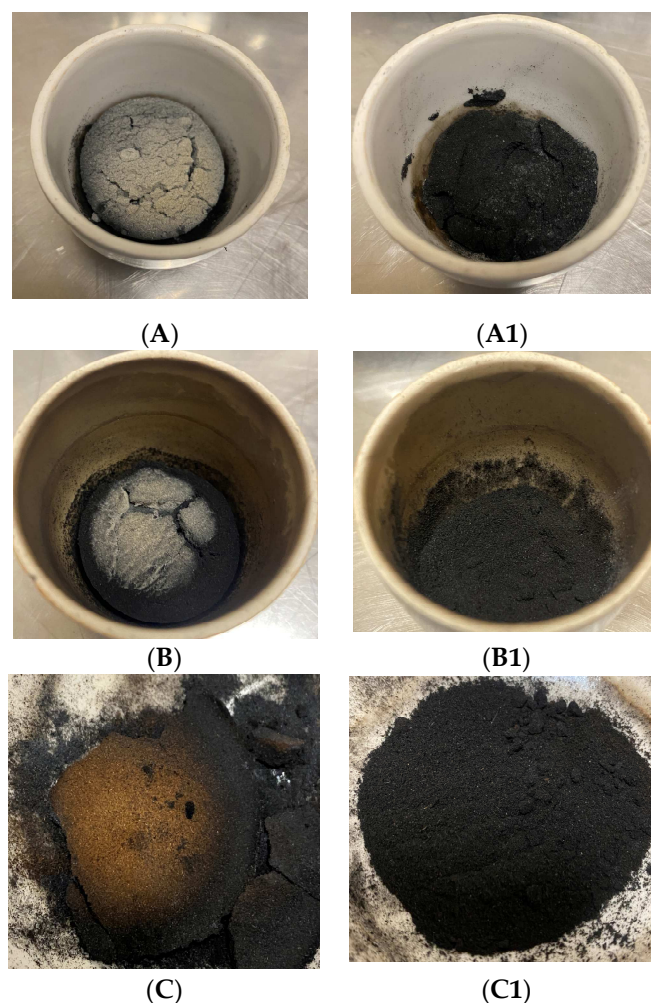
Figure 3. Bioadsorbents before and after ash removal; (**A**) BCT1, (**A1**) BCT1 without ash (**B**) BCT2, (**B1**) BCT2 without ash and (**C**) BCT3, (**C1**) BCT3 without ash.

3.2. Proximate Analysis of Biomass

The proximate analysis of biomass (Table 1), revealed moisture (1.94%), ash (9%), volatile matter (84.82%), and fixed carbon (4.24%). The low moisture content likely stems from the predrying process during biomass conditioning. Unlike some studies using nondried biomass, this approach may influence results [44]. The ash, volatile matter, and fixed carbon content fell within the average range documented for lignocellulosic materials like sugarcane bagasse, laurel sawdust, cinnamon, and eucalyptus [45]. Importantly, the high volatile matter content as noted by Velázquez's et al. [46] is advantageous for bioadsorbent production [47].

Table 1. Proximate analysis results of *Agave angustifolia* bagasse.

Proximate Analysis	Mass Percentage
Moisture	$1.94 \pm 0.154\%$
Ash	$9.00 \pm 0.100\%$
Volatile matter	$84.82 \pm 1.297\%$
Fixed carbon	$4.24 \pm 0.982\%$
Protein	$4.02 \pm 0.107\%$
Ethereal extract	$0.70 \pm 0.097\%$

3.3. Morphological Characterization (SEM) of Biomass and Bioadsorbents

SEM images (Figure 4) revealed that the bagasse exhibited fibers with perforations and a rough surface, suggesting the presence of macromolecules like cellulose, hemicellulose, and lignin [48]. Physical activation significantly altered the surface morphology of the bioadsorbents. The bagasse's holes and rough surface transformed into abundant irregular pores, indicating a highly porous structure. These porosity characteristics are crucial for contaminant removal materials as they provide a larger surface area, facilitating superior adsorption capacity [49].
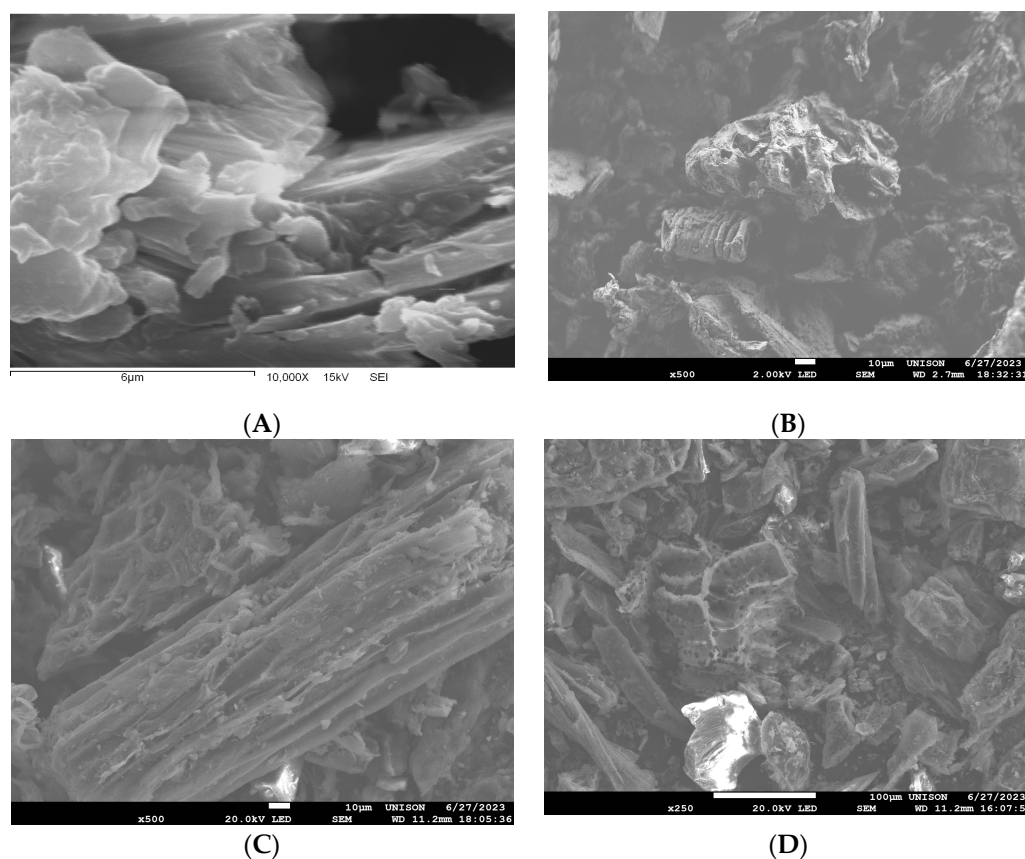

Figure 4. Scanning electron microscopy (SEM) of biomass and bioadsorbents. (**A**) *Agave angustifolia bagasse*, (**B**) BCT1, (**C**) BCT2, and (**D**) BCT3.

3.4. Biomass and Bioadsorbents Structural Characterization (FTIR)

Figure 5 presents the results of Fourier-transform infrared spectroscopy (FTIR) of biomass and bioadsorbents, highlighting key wavenumbers and their corresponding functional groups. The biomass spectrum displayed characteristic functional groups of hemicellulose (beta-glucosidic linkage of cellulose at 769 cm^{-1}) and lignin (aromatic rings at 1635 cm^{-1}). There was a strong intensity absorption peak at 3272 cm^{-1}, being attributed to the stretching of O-H bonds due to the presence of a hydroxyl group, while peaks at 2918 cm^{-1} indicated the presence of a C-H group, at 1616 cm^{-1} of absorbed O-H or carbonyl bands, at 1431 cm^{-1} of a $-CH_2$ group, at 1242 cm^{-1} of C-O bending of cellulose and hemicellulose, at 1027 cm^{-1} of a C-O bond, C-H bending bond and C-C stretching bond, at 773 cm^{-1} indicated the presence of β-glycosidic bond in cellulose or out-of-plane C-H bonds in lignin, and 595 cm^{-1} of carbon–carbon (C-C) bonds in the aromatic structures of lignin. In contrast, the bioabsorbents showed a decrease in intensity of higher wavenumbers, suggesting moisture loss due to high-temperature treatment. Furthermore, the absence of hemicellulose and cellulose bands implied their degradation at these temperatures [50]. Notably, the characteristic aromatic groups of lignin persisted in the

strong waves at 1410–1414 cm^{-1} and 1608 cm^{-1} (BCT1-3, respectively) [51]. This finding indicates that the carbonization process selectively degrades cellulose and hemicellulose, while preserving some lignin. This is advantageous because abundant lignin can contribute to high adsorption yield [52].
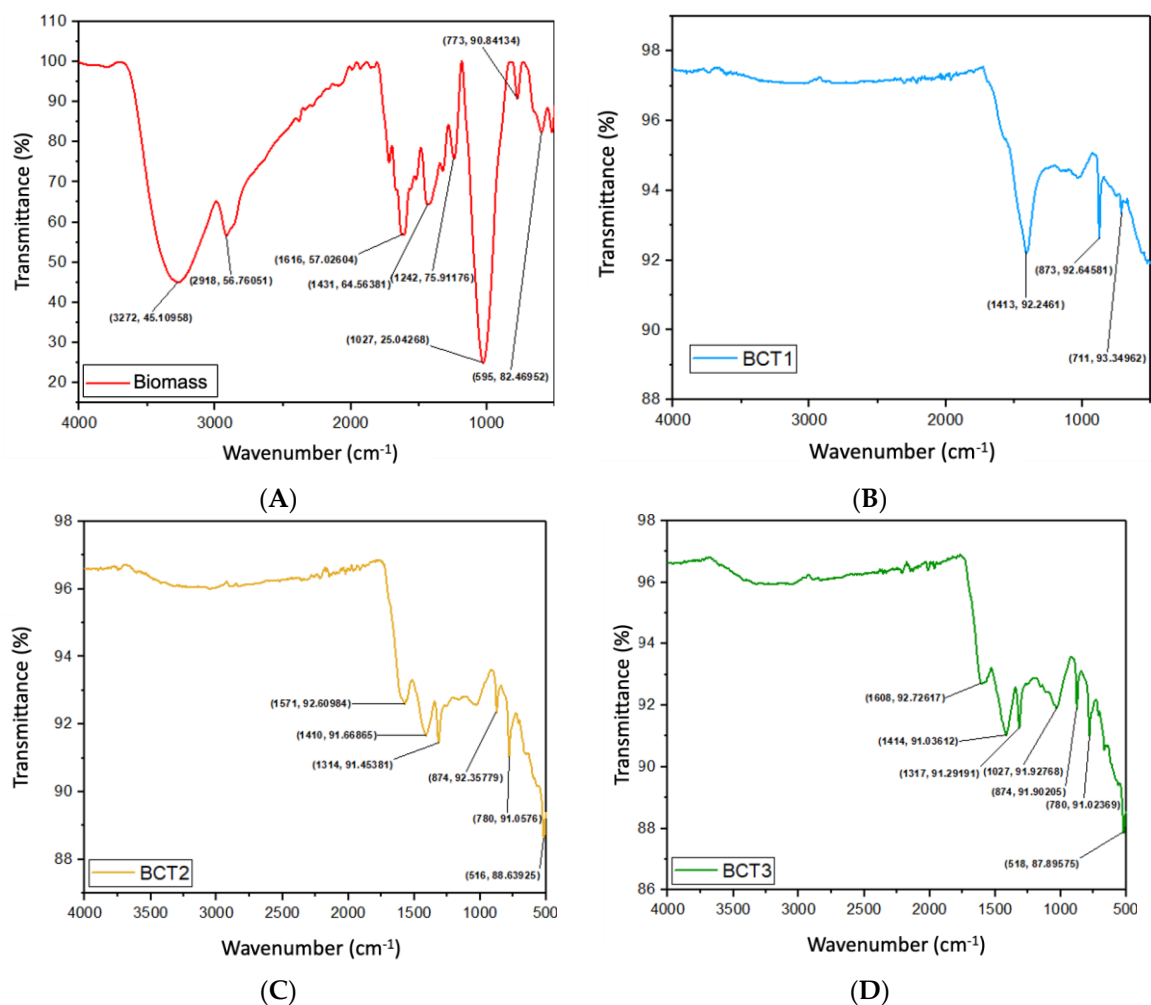

Figure 5. Fourier-transform infrared spectroscopy (FTIR) graphs of biomass and bioadsorbents. (**A**) *Agave angustifolia* bagasse, (**B**) BCT1, (**C**) BCT2, and (**D**) BCT3.

Lignin, a key component found in plant biomass such as wood and agricultural residues, plays a crucial role in the formation of the porous structure of biochar during the pyrolysis process (thermal decomposition in the absence of oxygen). Lignin is a complex polymer containing various functional groups, including hydroxyls and aromatic groups, which can interact with organic and inorganic contaminants in the environment. Due to this chemical structure, lignin exhibits high adsorption capacity, meaning it can bind to and retain contaminants on its surface. When lignin-rich biomass is used to produce biochar, the resulting product has a higher lignin content in its composition. This increased lignin content directly contributes to a higher adsorption capacity of the biochar. Therefore, in a biochar, a greater presence of lignin implies a greater potential to adsorb and retain contaminants from soil, water, or air, making it advantageous for environmental remediation and water purification purposes [52–54].

3.5. Thermal Analysis

3.5.1. Thermogravimetric Analysis (TGA) of Biomass and Bioadsorbents

TGA thermograms showed a nearly 10% mass loss between 100 °C and 200 °C, corresponding to moisture evaporation (Figure 6). A second mass decrease around 390–400 °C indicated cellulose and hemicellulose degradation [55]. Further mass loss (below 10% remaining) between 400 °C and 700 °C was attributed to lignin decomposition [56,57]. While bioadsorbents were not entirely degraded at 700 °C, BCT2 and BCT3 exhibited a weight reduction from 350 °C to 700 °C. Notably, BCT1 displayed only a 25% mass decrease, suggesting the least material degradation among the bioadsorbents. This observation aligns with the DTG curves, where BCT1 showed a single degradation peak, while BCT2 and BCT3 exhibited three and four peaks, respectively.
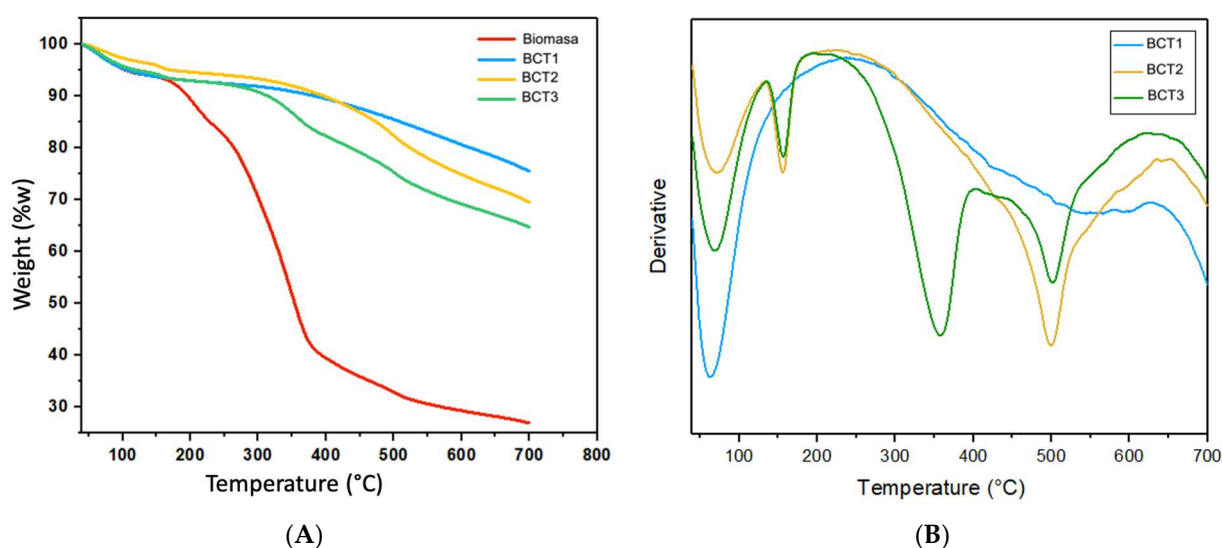

Figure 6. Thermograms of TGA, (**A**) *Agave angustifolia* Bagasse, BCT1, BCT2, and BCT3; and (**B**) derivative BCT1, BCT2, and BCT3.

The presence of a large peak in the derivative before 100 °C in a thermogravimetric analysis (TGA) of the bioadsorbent (BTC1 biochar) typically indicates the release of adsorbed or free water present in the sample. This phenomenon can be attributed to several factors. Firstly, the bioadsorbent's porous nature allows it to adsorb water from the surrounding environment, which is rapidly evaporated upon heating, manifesting as a weight loss peak in the TGA derivative. Additionally, free water trapped within the pores or structure of the bioadsorbent contributes to this initial weight loss. Furthermore, residual volatile compounds from the production process or precursor materials may also evaporate at relatively low temperatures, further adding to the observed peak in the TGA derivative [58].

3.5.2. Differential Scanning Calorimetry (DSC)

Figure 7 shows a differential scanning calorimetry (DSC) thermogram of *Agave angustifolia* bagasse biomass and bioadsorbents after the pyrolysis of lignocellulosic material; peaks observed at 40 °C, 160 °C, and 200 °C likely correspond to distinct thermal degradation phases. The peak at 40 °C (initial water desorption temperature) likely signifies the desorption of moisture or water present within the material's pores in biomass and bioadsorbents [59]. At 160 °C (decomposition temperature of organic matter) in biomass, BCT2, and BCT3, the peak suggests the onset of decomposition for organic components such as cellulose and hemicellulose, releasing volatile compounds and altering the system's specific heat capacity, similarly to the findings of De Dios Naranjo et al. [60], where fibers from *Agave salmiana* showed endotherms at 110 °C and 139 °C. A common observation across the bioadsorbents BCT2 and BCT3 was cellulose degradation at around 200 °C,

aligning with findings on sugarcane bagasse by Bernardino et al. [61]. Interestingly, BCT1 did not exhibit any additional phase transitions as seen in Figure 7.
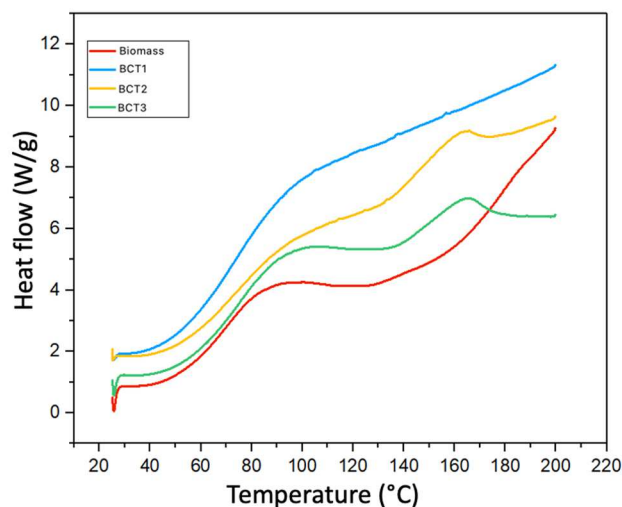

Figure 7. DSC thermograms of biomass, BCT1, BCT2, and BCT3.

3.6. Preliminary Adsorption Tests

BCT1 and BCT2 achieved complete ibuprofen removal (100%) at pH 2 after 48 h with an agitation speed of 150 rpm, suggesting surface properties compatible with ibuprofen adsorption. These bioadsorbents likely possess a combination of functional groups, such as hydroxyl, carboxyl, ether, and amide, among others, as well as surface radicals and surface charge that are compatible with ibuprofen molecules that facilitate adsorption of molecules with similar structures [62]. Figure 8 visually depicts the changes in the microstructure of these bioadsorbents before and after adsorption. While SEM and FTIR analyses of BCT3 after adsorption supported potential adsorption, further testing is necessary due to inconsistencies in specific adsorption test readings.
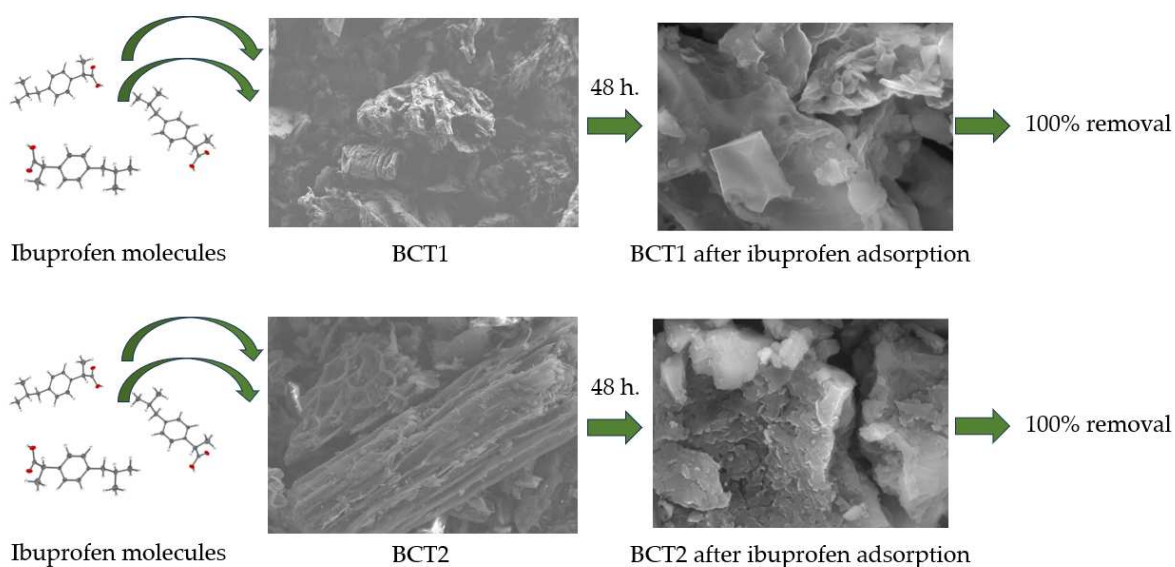

Figure 8. Adsorption process of ibuprofen on bioadsorbents BCT1 and BCT2.

4. Discussion

4.1. Bioadsorbent Structure

The characterization results revealed that the bioadsorbents derived from *Agave angustifolia bagasse* exhibited a porous structure with a high surface area, which is desirable

for adsorption applications. The presence of functional groups on the biochar surface, as identified via FTIR analysis, suggests its potential for interacting with target contaminants like ibuprofen. Other similar studies have been carried out to remove pollutants in an aquatic environment, such as the research presented by Liu et al. [63]. The bioadsorbents prepared by Chladophora (CB) were used to adsorb the ibuprofen and ofloxacin in sewage. SEM showed that CB preserved the natural tubular structure and increased its specific surface area. According to the BET results, the specific surface area of CB was 296.831 m^2 g^{-1}. The adsorption of ibuprofen and ofloxacin on biochar conformed to the pseudo second-order kinetic model, indicating that their adsorption rate was controlled via the chemical adsorption mechanism. The bioadsorbents obtained from *Agave angustifolia* bagasse presented better ibuprofen removal results than the bioadsorbent result from Chladophora, due to the characteristics of the material and functional groups present on the surface. Nama et al. [64] produced bioadsorbent from a commercially significant microalga, such as Dunaliella biomass, through pyrolysis. FT-IR was employed to examine both the morphological and functional aspects of the biochar, as well as its thermal degradation behavior. Pyrolytic behavior was further explored using thermogravimetric analysis under an oxidizing environment. SEM analysis revealed diverse and rough-textured structures of the biochar, supporting enhanced adsorption capabilities. The biochar was used to remove naphthalene in aquatic environments, obtaining a removal of 63% of 100 mg L^{-1} of the pollutant. The structure of the bioadsorbents obtained by Nama et al. [64] was similar to that obtained in the present study for *Agave angustifolia* bioadsorbents.

4.2. Demonstration of the Functionality of Bioadsorbents

SEM images (Figure 9) revealed significant changes in the morphology of the postadsorption bioadsorbents (BCCT1, BCCT2, BCCT3) compared to their initial structure. All three displayed a grayish layer obstructing pores, with BCCT1 and BCCT3 exhibiting a reduction in the number of pores. Interestingly, BCCT2 showed a reduced surface roughness, indicating ibuprofen incorporation on its surface. These observations align with previous studies reporting similar postadsorption characteristics, supporting the efficiency of the adsorption process [65,66]. The adsorption performance of bioadsorbents depended on the reaction conditions, including the raw materials used, kinetic parameters, pH value, and specific surface area.

Figure 10 shows the infrared spectrum of ibuprofen (Figure 10A) and the infrared spectra of the bioadsorbents after removal of ibuprofen (Figure 10B–D). The analysis of infrared spectra (FTIR) provides valuable information about molecular structure and interactions present in the chemical compounds under study. Starting with the spectra of ibuprofen and the bioadsorbents derived from *Agave angustifolia* bagasse, characteristic bands were identified that reveal specific bond vibrations. In the ibuprofen spectrum, the bands at 2362 cm^{-1} and 2302 cm^{-1} are attributed to the stretching vibrations of the carboxyl (C=O) and C=C functional groups, respectively. The band at 1618 cm^{-1} corresponds to the bending vibration of the aromatic ring. The values of 1710–1708 cm^{-1} correspond to the vibration of the ester functional group (–COO–), specifically the carbonyl bond (–C=O), which is present in the structure of ibuprofen. The bands at 1314 cm^{-1} and 1160 cm^{-1} are associated with the stretching vibrations of C–O and C–C bonds, respectively, and are indicative of the presence of ester and alkyl groups in the ibuprofen molecule. The bands at 1034 cm^{-1}, 778 cm^{-1}, and 514 cm^{-1} are related to characteristic vibrations of the aromatic structure and C-H bond in the ibuprofen spectrum.

In the spectra of bioadsorbents (BCCT1, BCCT2, and BCCT3), bands suggesting the presence of different functional groups were observed. Intense bands in the 3700–2900 cm^{-1} region are typical of the stretching vibrations of –OH and –CH groups present in organic compounds. The bands at 2154 cm^{-1}, 2006 cm^{-1}, and 1948 cm^{-1} may be related to vibrations of C≡C bonds. In the three bioadsorbents, the spectra showed the band at 1710–1708 cm^{-1} (inverted) and 1610–1598 cm^{-1} corresponding to the carbonyl carbon (–C=O) of the carboxyl group of ibuprofen. Also, the band at 1598 cm^{-1} indicates the

presence of double C=C bonds in carbonaceous structures. The band at 1434–1402 cm^{-1} may be related to the bending vibration of the –C–H bond in alkenes and aromatic rings of the bioadsorbent and ibuprofen. The bands at 1324 cm^{-1} and 1168 cm^{-1} correspond to the stretching vibrations of C–O and C–C, respectively, similar to those observed in the ibuprofen spectrum.
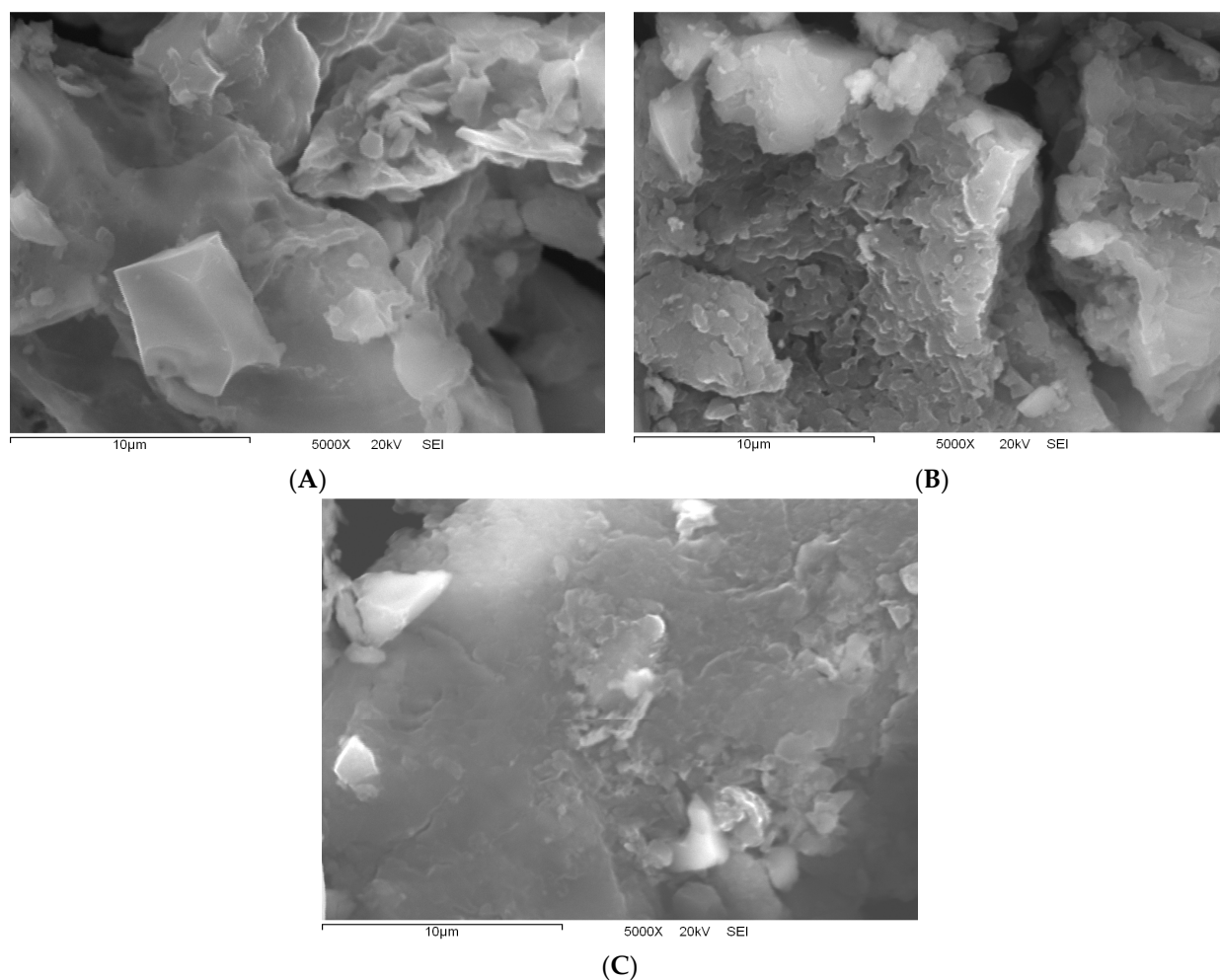

Figure 9. Scanning electron microscopy (SEM) of bioadsorbents after adsorption test. (**A**) BCCT1, (**B**) BCCT2, and (**C**) BCCT3.

The overlap of ibuprofen bands in the spectra of the bioadsorbents suggests an interaction between the drug and the adsorbent material. Adsorption mechanisms likely involve a combination of hydrophobic interactions, hydrogen bonding, and π-π interactions between the benzene ring of ibuprofen and the carbonaceous structures of the bioadsorbents. The presence of functional groups on the surface of the bioadsorbents, such as –OH and –COOH, facilitates hydrogen bonding interactions with the functional groups of ibuprofen, while π-π interactions benefit from the aromatic structure of both components. These observations indicate effective adsorption of ibuprofen molecules on the bioadsorbent surface through interactions with functional groups, as evidenced by the presence of characteristic ibuprofen bands [67].

The difference in adsorption capacity among the three bioadsorbents can be attributed to variations in chemical composition and surface morphology. For example, the presence of specific functional groups such as hydroxyl (–OH) or carboxyl (–COOH) groups may increase the bioadsorbents affinity for ibuprofen through hydrogen bonding interactions. Additionally, differences in pore structure and specific surface area of each bioadsorbent

may influence the amount of available adsorption sites. Overall, the bioadsorbent exhibiting a higher quantity of functional groups and a greater surface area is expected to have a higher adsorption capacity for ibuprofen, such as BCCT1 and BBCT2 bioadsorbents.
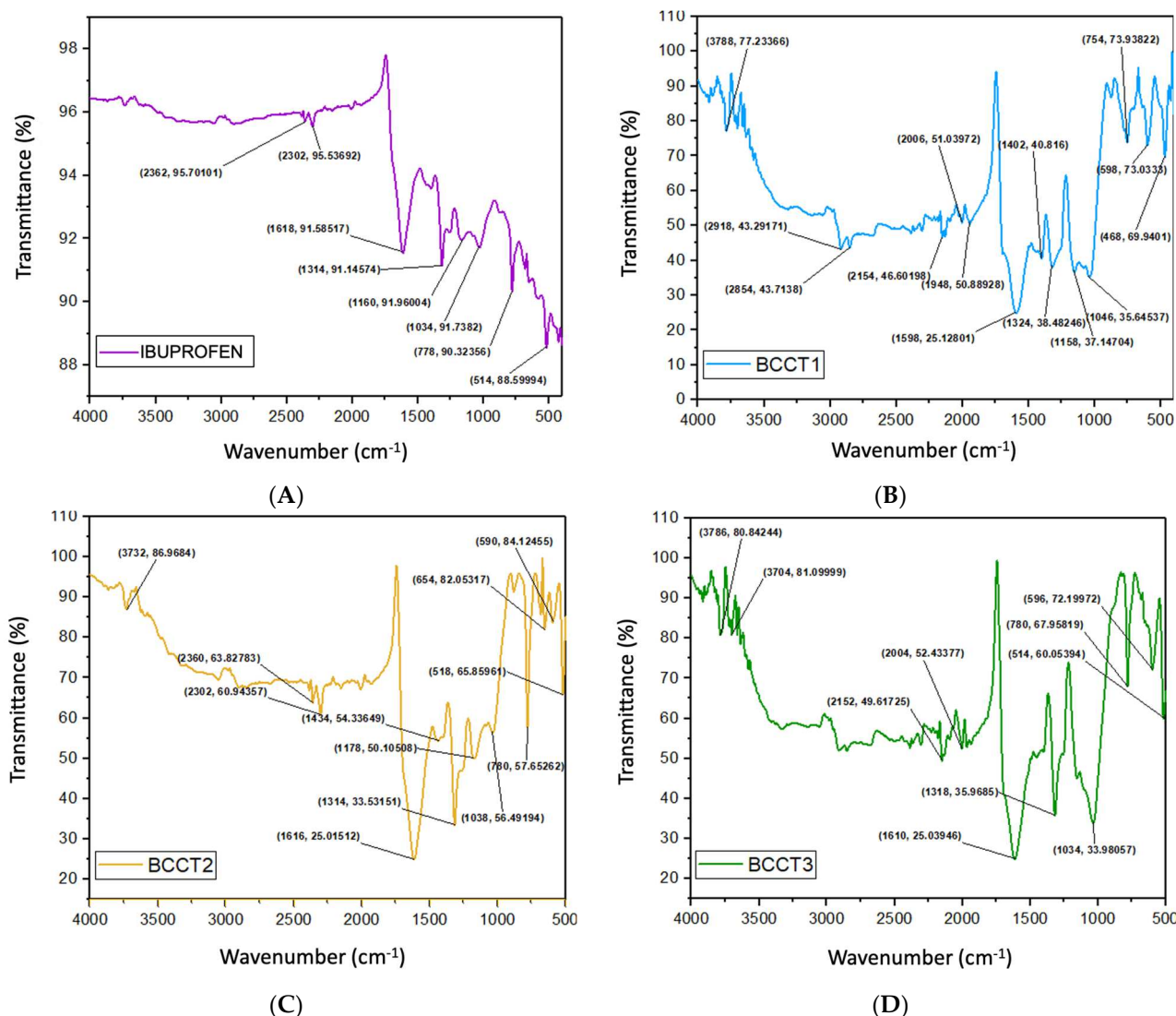

Figure 10. Fourier-transform infrared spectroscopy (FTIR) graphs of ibuprofen and bioadsorbents after adsorption test. (**A**) Ibuprofen, (**B**) BCCT1, (**C**) BCCT2, and (**D**) BCCT3.

The interaction mechanisms between biochar and pollutants in water exhibit diversity, encompassing physical adsorption, chemical adsorption, redox, and microbial activity. With numerous micropores and mesopores, biochar effectively absorbs dissolved pollutants. Moreover, its high specific surface area offers ample adsorption sites for a range of compounds, including organic pollutants, heavy metals, and nitrogen oxides. Beyond physical adsorption, biochar demonstrates chemical adsorption capabilities through surface functional groups forming covalent or hydrogen bonds with contaminants. Additionally, biochar engages in redox reactions, facilitating the conversion of pollutants into harmless substances through chemical reduction or oxidation. The efficacy of biochar in adsorbing and removing pollutants like ibuprofen varies depending on the material and its adsorption mechanism [68].

Specifically, the absorption of ibuprofen into biochar varies depending on the material used. Various studies have elucidated the mechanisms underlying ibuprofen by adsorption onto biochar. The mechanisms of absorption and removal of ibuprofen via biochar en-

compass a variety of processes. These include multimolecular adsorption, π-π interaction, pore filling, hydrogen bonding, and interactions between π-acceptors and electrostatics. Additionally, the application of pseudo-second-order kinetics and Langmuir–Freundlich isotherm models in adsorption was observed. Mechanisms such as pore filling-diffusion, hydrophobic interaction, and π-π electron donor-acceptor interaction also contribute to ibuprofen removal. Improved adsorption and separation were achieved through the preparation of magnetic biochar, while stability across multiple adsorption cycles was evidenced in successful biochar reuse. These findings underscore the efficacy and versatility of biocarbon derived from biomass waste in environmentally friendly and economically viable ibuprofen removal in aqueous environments [68–70].

To examine the adsorption capacity of a material, researchers primarily use batch experiments. In batch experiments, the design typically encompasses several stages. First, the material undergoes preparation, which may involve raw biomass, chemically modified biomass, or thermal treatment to produce biochars, among other methods. Next, various experimental parameters such as initial and final pH of the solution, contact time, initial concentration of the pollutant, ionic strength, particle size of the adsorbent, and dose of adsorbent are studied and optimized. Subsequently, the adsorption mechanism is investigated, followed by desorption experiments to assess the release of adsorbed pollutants. Finally, the potential for regeneration and reusability of the material is evaluated [71], these last two points being a limitation of the present study.

4.3. Contribution of the Study to Sustainability

The presence of pharmaceutical residues in the environment, including ibuprofen, poses a significant threat to ecosystems. According to the FAO and UNEP [72], over 4000 widely used pharmaceutical and chemical products, including drugs, contribute to environmental pollution and the emergence of drug-resistant diseases. Furthermore, soil pollution is intrinsically linked to the degradation and loss of aquatic and terrestrial resources, impacting Sustainable Development Goals (SDGs) 14 (life below water) and 15 (life on land) [72–74]. In this sense, developing effective methods for managing pharmaceutical residues is critical to achieve a more sustainable future.

Also, the study exploration of utilizing bacanora industry bagasse for biochar production represents a significant contribution to sustainability efforts. By repurposing this byproduct, the research not only addresses waste management concerns but also offers a viable solution for mitigating emerging pollution, such as pharmaceutical residues. Biochar derived from bacanora bagasse has the potential to effectively remove these pharmaceutical residues from various environmental matrices, thereby promoting cleaner ecosystems and healthier communities. This innovative approach highlights the intersection of agricultural industry byproducts and environmental stewardship, showcasing how sustainable practices can emerge from unlikely sources.

5. Conclusions

Agave angustifolia bagasse exhibits great potential as a pyrolysis-derived adsorbent (yield: 25.65–38.28%) for ibuprofen removal. Both biomass and bioadsorbents (BCT1, BCT2, and BCT3) possessed functional groups associated with cellulose, hemicellulose, and lignin. These macromolecules underwent degradation at around 350 °C (cellulose and hemicellulose), while lignin remained partially undegraded at 550 °C. While biomass displayed a fissured and porous morphology, bioadsorbents displayed a highly porous surface. After the adsorption process, these surfaces showed surface coverage consistent with ibuprofen adsorption. Treatments BCT1 and BCT2 successfully removed 100% of ibuprofen from an aqueous solution with an initial concentration of 62.5 mg/L. Supplementary adsorption tests are needed for BCT3, as SEM and FTIR results suggest successful adsorption despite inconsistent readings in specific adsorption tests. Overall, bioadsorbents derived from *Agave angustifolia* bagasse biomass demonstrate significant potential for the removal of ibuprofen from aqueous solutions.

References

1. Nwokediegwu, Z.Q.S.; Daraojimba, O.H.; Oliha, J.S.; Obaigbena, A.; Dada, M.A.; Majemite, M.T. Review of emerging contaminants in water: USA and African perspectives. *Int. J. Sci. Res. Arch.* **2024**, *11*, 350–360. [CrossRef]
2. Thi, L.A.P.; Ly, L.T.M.; Do, H.T.; Chinh, P.M. Occurrence and risks of emerging pollutants in water bodies. In *Advanced Functional Materials and Methods for Photodegradation of Toxic Pollutants*; Elsevier: Amsterdam, The Netherlands, 2024; pp. 1–36. [CrossRef]
3. Munzhelele, E.P.; Mudzielwana, R.; Ayinde, W.B.; Gitari, W.M. Pharmaceutical Contaminants in Wastewater and Receiving Water Bodies of South Africa: A Review of Sources, Pathways, Occurrence, Effects, and Geographical Distribution. *Water* **2024**, *16*, 796. [CrossRef]
4. Fraiha, O.; Hadoudi, N.; Zaki, N.; Salhi, A.; Amhamdi, H.; Akichouh, E.H.; Mourabit, F.; Ahari, M. Comprehensive review on the adsorption of pharmaceutical products from wastewater by clay materials. *Desalination Water Treat.* **2024**, *317*, 100114. [CrossRef]
5. Puri, M.; Gandhi, K.; Kumar, M.S. Emerging environmental contaminants: A global perspective on policies and regulations. *J. Environ. Manag.* **2023**, *332*, 117344. [CrossRef]
6. Nain, P.; Anctil, A. End-of-life solar photovoltaic waste management: A comparison as per European Union and United States regulatory approaches. *Resour. Conserv. Recycl. Adv.* **2024**, *21*, 200212. [CrossRef]
7. Rainsford, K.D. Ibuprofen: Pharmacology, efficacy and safety. *Inflammopharmacology* **2009**, *17*, 275–342. [CrossRef]
8. Buser, H.-R.; Poiger, T.; Müller, M.D. Occurrence and Environmental Behavior of the Chiral Pharmaceutical Drug Ibuprofen in Surface Waters and in Wastewater. *Environ. Sci. Technol.* **1999**, *33*, 2529–2535. [CrossRef]
9. Marchlewicz, A.; Guzik, U.; Wojcieszyńska, D. Over-the-Counter Monocyclic Non-Steroidal Anti-Inflammatory Drugs in Environment—Sources, Risks, Biodegradation. *Water Air Soil Pollut.* **2015**, *226*, 355. [CrossRef]
10. Muñiz-González, A.-B. Ibuprofen as an emerging pollutant on non-target aquatic invertebrates: Effects on Chironomus riparius. *Environ. Toxicol. Pharmacol.* **2021**, *81*, 103537. [CrossRef]
11. Parolini, M.; Binelli, A.; Provini, A. Chronic effects induced by ibuprofen on the freshwater bivalve Dreissena polymorpha. *Ecotoxicol. Environ. Saf.* **2011**, *74*, 1586–1594. [CrossRef]
12. Chopra, S.; Kumar, D. Ibuprofen as an emerging organic contaminant in environment, distribution and remediation. *Heliyon* **2020**, *6*, e04087. [CrossRef] [PubMed]
13. Jan-Roblero, J.; Cruz-Maya, J.A. Ibuprofen: Toxicology and Biodegradation of an Emerging Contaminant. *Molecules* **2023**, *28*, 2097. [CrossRef] [PubMed]
14. Dey Chowdhury, S.; Surampalli, R.Y.; Bhunia, P. Advanced Oxidation Processes for Microconstituents Removal in Aquatic Environments. In *Microconstituents in the Environment: Occurrence, Fate, Removal and Management*; John Wiley & Sons, Inc.: Hoboken, NJ, USA, 2023; pp. 367–404. [CrossRef]
15. Zhao, S.; Li, H.; Zhou, J.; Sumpradit, T.; Salama, E.-S.; Li, X.; Qu, J. Simultaneous degradation of NSAIDs in aqueous and sludge stages by an electron-Fenton system derived from sediment microbial fuel cell based on a novel Fe@Mn biochar GDC. *Chem. Eng. J.* **2024**, *482*, 148979. [CrossRef]
16. Zamora, J.; Rodríguez, M.; Vera, L.; Gómez, Y. Técnicas aplicadas a la remoción de fármacos, usados en el tratamiento del COVID-19: Una revisión. *Polo Del Conoc.* **2021**, *6*, 15–36.
17. Qiu, X.; Wang, B.; Zhao, X.; Zhou, X.; Wang, R. Green and Sustainable Imprinting Technology for Removal of Heavy Metal Ions from Water via Selective Adsorption. *Sustainability* **2023**, *16*, 339. [CrossRef]
18. El-Taweel, R.M.; Mohamed, N.; Alrefaey, K.A.; Husien, S.; Abdel-Aziz, A.; Salim, A.I.; Mostafa, N.G.; Said, L.A.; Fahim, I.S.; Radwan, A.G. A review of coagulation explaining its definition, mechanism, coagulant types, and optimization models; RSM, and ANN. *Curr. Res. Green Sustain. Chem.* **2023**, *6*, 100358. [CrossRef]

19. Verma, A.; Sharma, G.; Kumar, A.; Dhiman, P.; Mola, G.T.; Shan, A.; Si, C. Microplastic pollutants in water: A comprehensive review on their remediation by adsorption using various adsorbents. *Chemosphere* **2024**, *352*, 141365. [CrossRef] [PubMed]

20. Wang, Y.; Chen, L.; Zhu, Y.; Fang, W.; Tan, Y.; He, Z.; Liao, H. Research status, trends, and mechanisms of biochar adsorption for wastewater treatment: A scientometric review. *Environ. Sci. Eur.* **2024**, *36*, 25. [CrossRef]

21. Hu, B.; Ai, Y.; Jin, J.; Hayat, T.; Alsaedi, A.; Zhuang, L.; Wang, X. Efficient elimination of organic and inorganic pollutants by biochar and biochar-based materials. *Biochar* **2020**, *2*, 47–64. [CrossRef]

22. Li, R.; Zhang, C.; Chen, W.-H.; Kwon, E.E.; Rajendran, S.; Zhang, Y. Multistage utilization of soybean straw-derived P-doped biochar for aquatic pollutant removal and biofuel usage. *Bioresour. Technol.* **2023**, *387*, 129657. [CrossRef]

23. Janiszewska, D.; Olchowski, R.; Nowicka, A.; Zborowska, M.; Marszalkiewicz, K.; Shams, M.; Giannakoudakis, D.A.; Anastopoulos, I.; Barczak, M. Activated biochars derived from wood biomass liquefaction residues for effective removal of hazardous hexavalent chromium from aquatic environments. *GCB Bioenergy* **2021**, *13*, 1247–1259. [CrossRef]

24. Ali, I.; Asim, M.; Khan, T.A. Low cost adsorbents for the removal of organic pollutants from wastewater. *J. Environ. Manag.* **2012**, *113*, 170–183. [CrossRef]

25. Homem, V.; Santos, L. Degradation and removal methods of antibiotics from aqueous matrices—A review. *J. Environ. Manag.* **2011**, *92*, 2304–2347. [CrossRef] [PubMed]

26. Sherpa, S.W.; Ponnuchamy, M.; Kapoor, A.; Jacob, M.M.; Sivaraman, P. Facile removal of sulfamethoxazole antibiotic from contaminated water using bagasse-derived pyrolytic biocarbon: Parametric assessment, mechanistic insights and scale-up analysis. *J. Water Process. Eng.* **2024**, *60*, 105110. [CrossRef]

27. Clavero, V.O.; Weber, A.; Schröder, W.; Curticapean, D. Spectral analysis of bacanora (agave-derived liquor) by using FT-Raman spectroscopy. In *Optical Sensing and Detection IV*; SPIE: Bellingham, WA, USA, 2016; Volume 9899, pp. 618–625. [CrossRef]

28. Salazar, V. La industria del bacanora: Historia y tradición de resistencia en la sierra sonorense. *Reg. Soc.* **2007**, *19*, 105–133. [CrossRef]

29. Cortés, C. Propiedades Mecánicas a Tensión de las Fibras del Bagazo del Agave Angustifolia Haw, Residuo Proveniente de la Producción Artesanal del Mezcal. Master's Thesis, Instituto Politécnico Nacional, Mexico City, Mexico, 2009.

30. Sierra, E.; Alcaraz, J.; Valdivia, A.; Rosas, A.; Hernández, M.; Vivaldo, E.; Martínez, A. Bagazo de Agave: De Desecho Agroindustrial a Materia Prima en las Biorrefinerías. Universidad Autónoma de México. 2021. Available online: http://ciencia.unam.mx/leer/1112/bagazo-de-agave-de-desecho-agroindustrial-a-materia-prima-en-las-biorrefinerias- (accessed on 3 February 2024).

31. Hidalgo-Reyes, M.; Caballero-Caballero, M.; Hernández-Gómez, L.H.; Urriolagoitia-Calderón, G. Chemical and morphological characterization of Agave angustifolia bagasse fibers. *Bot. Sci.* **2015**, *93*, 807–817. [CrossRef]

32. Jiménez-Ortega, L.A.; Valdez-Baro, O.; Bernal-Millán, M.J.; Rivera-Salas, M.M.; Heredia, J.B. Agave Byproducts: As Sources of Phytochemicals with Functional Activities and Their Management for Industrial Applications. In *Food Byproducts Management and Their Utilization*; Apple Academic Press: Palm Bay, FL, USA, 2024; pp. 385–416. [CrossRef]

33. Gómora-Hernández, J.C.; Tecante, A.; del Carmen Carreño-De-León, M.; Flores-Álamo, N.; Ventura-Cruz, S. Preparation of porous microcrystalline cellulose from mezcal industry agave bagasse by low reagent loading sequential chemical treatment. *Cellulose* **2023**, *30*, 2067–2084. [CrossRef]

34. Ayala-Cortés, A.; Arancibia-Bulnes, C.A.; Villafán-Vidales, H.I.; Lobato-Peralta, D.R.; Martínez-Casillas, D.C.; Cuentas-Gallegos, A.K. Solar pyrolysis of agave and tomato pruning wastes: Insights of the effect of pyrolysis operation parameters on the physicochemical properties of biochar. *AIP Conf. Proc.* **2019**, *2126*, 180001. [CrossRef]

35. Lobato-Peralta, D.R.; Ayala-Cortes, A.; Longoria, A.; Pacheco-Catalan, D.E.; Okoye, P.U.; Villafan-Vidales, H.I.; Arancibia-Bulnes, C.A.; Cuentas-Gallegos, A.K. Activated carbons obtained by environmentally friendly activation using solar energy for their use in neutral electrolyte supercapacitors. *J. Energy Storage* **2022**, *52*, 104888. [CrossRef]

36. Robles-García, M.; Del-Toro-Sánchez, C.L.; Márquez-Ríos, E.; Barrera-Rodríguez, A.; Aguilar, J.; Aguilar, J.A.; Reynoso-Marín, F.J.; Ceja, I.; Dórame-Miranda, R.; Rodríguez-Félix, F. Nanofibers of cellulose bagasse from Agave tequilana Weber var. azul by electrospinning: Preparation and characterization. *Carbohydr. Polym.* **2018**, *192*, 69–74. [CrossRef]

37. NORMA Oficial Mexicana. *NOM-116-SSA1-1994, Determinación de Humedad en Alimentos por Tratamiento Térmico. Método por Arena o Gasa*; Pub. L. No. 116; Diario Oficial de la Federación: Mexico City, Mexico, 1994.

38. Proyecto de Norma Mexicana PROY-NMX-F-607-NORMEX-2020. *Determinación de Cenizas en Alimentos-Método de Prueba*; Diario Oficial de la Federación: Mexico City, Mexico, 2020.

39. U.S. Department of Energy. *Standard Test Method for Volatile Matter in the Analysis of Particulate Wood Fuels*; ASTM International: West Conshohocken, PA, USA, 2019.

40. Martínez, A.; Bohórquez, L. *Evaluación de la Eficiencia de Biochar Producido a Partir de Pirólisis Lenta de Bagazo de Caña Como Medio Filtrante Para Retención de Fenoles en Matriz Acuosa [Monography]*; Universidad de La Salle: Bogotá, Colombia, 2017.

41. Williams, P.T.; Nugranad, N. Comparison of products from the pyrolysis and catalytic pyrolysis of rice husks. *Energy* **2000**, *25*, 493–513. [CrossRef]

42. Iglesias-Abad, S.; Alvarez-Vera, M.; Salas, C.; Vázquez, J. Biochar of residual biomass from eucalyptus (*Eucalyptus globulus*) by two pyrolysis methods. *Manglar* **2020**, *17*, 105–111. [CrossRef]

43. Cha, J.S.; Park, S.H.; Jung, S.-C.; Ryu, C.; Jeon, J.-K.; Shin, M.-C.; Park, Y.-K. Production and utilization of biochar: A review. *J. Ind. Eng. Chem.* **2016**, *40*, 1–15. [CrossRef]

44. Flores, P.; Robles, C.; Castañeda, E. Generación y caracterización básica de bagazos de la agroindustria del mezcal en Oaxaca. *Rev. Mex. Cienc. Agrícolas* **2020**, *11*, 1437–1445. [CrossRef]

45. Asimbaya, C.; Rosas, N.; Endara, D.; Guerrero, V. Obtención de Carbón Activado a partir de Residuos Lignocelulósicos de Canelo, Laurel y Eucalipto. *Rev. Politécnica* **2016**, *36*, 24.

46. Velázquez, A.; Bolaños, E.; Pliego, Y. Optimización de la Producción de Carbón Activado a Partir de Bambú. *Rev. Mex. Ing. Química* **2010**, *9*, 359–366.

47. Alonso, M.; Rigal, L. Caracterización y valorización del bagazo de Agave tequilana Weber de la industria del tequila. *Rev. Chapingo* **1997**, *3*, 31–39. [CrossRef]

48. Azeh, Y.; Olatunji, G.A.; Mamza, P.A. Scanning Electron Microscopy and Kinetic Studies of Ketene-Acetylated Wood/Cellulose High-Density Polyethylene Blends. *Int. J. Carbohydr. Chem.* **2012**, *2012*, 456491. [CrossRef]

49. Weber, K.; Quicker, P. Properties of biochar. *Fuel* **2018**, *217*, 240–261. [CrossRef]

50. Wang, J.; Minami, E.; Asmadi, M.; Kawamoto, H. Effect of delignification on thermal degradation reactivities of hemicellulose and cellulose in wood cell walls. *J. Wood Sci.* **2021**, *67*, 19. [CrossRef]

51. Janu, R.; Mrlik, V.; Ribitsch, D.; Hofman, J.; Sedláček, P.; Bielská, L.; Soja, G. Biochar surface functional groups as affected by biomass feedstock, biochar composition and pyrolysis temperature. *Carbon Resour. Convers.* **2021**, *4*, 36–46. [CrossRef]

52. Hu, J.; Shen, D.; Wu, S.; Zhang, H.; Xiao, R. Effect of temperature on structure evolution in char from hydrothermal degradation of lignin. *J. Anal. Appl. Pyrolysis* **2014**, *106*, 118–124. [CrossRef]

53. Gul, E.; Alrawashdeh, K.A.B.; Masek, O.; Skreiberg, Ø.; Corona, A.; Zampilli, M.; Wang, L.; Samaras, P.; Yang, Q.; Zhou, H.; et al. Production and use of biochar from lignin and lignin-rich residues (such as digestate and olive stones) for wastewater treatment. *J. Anal. Appl. Pyrolysis* **2021**, *158*, 105263. [CrossRef]

54. Li, Y.; Wang, F.; Miao, Y.; Mai, Y.; Li, H.; Chen, X.; Chen, J. A lignin-biochar with high oxygen-containing groups for adsorbing lead ion prepared by simultaneous oxidization and carbonization. *Bioresour. Technol.* **2020**, *307*, 123165. [CrossRef]

55. Tripathi, M.; Sahu, J.; Ganesan, P. Effect of process parameters on production of biochar from biomass waste through pyrolysis: A review. *Renew. Sustain. Energy Rev.* **2016**, *55*, 467–481. [CrossRef]

56. Pereira, M.E.; Varanda, L.D.; de Carvalho, N.R.; Sette, C., Jr.; de Padua, F.A.; De Conti, A.C.; Yamaji, F.M. Biochar produced from poultry litter waste. *Res. Soc. Dev.* **2021**, *10*, e351101119704. [CrossRef]

57. De la Cuesta, J.; Montoya, U.; Betancourt, S.; Álvarez, C. Effect of processing temperature on the mechanical properties of binderless fiberboards. *Prospect* **2011**, *9*, 75–80.

58. Rasapoor, M.; Young, B.; Asadov, A.; Brar, R.; Sarmah, A.K.; Zhuang, W.-Q.; Baroutian, S. Effects of biochar and activated carbon on biogas generation: A thermogravimetric and chemical analysis approach. *Energy Convers. Manag.* **2020**, *203*, 112221. [CrossRef]

59. El-Nemr, M.A.; Abdelmonem, N.M.; Ismail, I.M.A.; Ragab, S.; El Nemr, A. Ozone and Ammonium Hydroxide Modification of Biochar Prepared from *Pisum sativum* Peels Improves the Adsorption of Copper (II) from an Aqueous Medium. *Environ. Process.* **2020**, *7*, 973–1007. [CrossRef]

60. De Dios Naranjo, C.; Alamilla, L.; Gutiérrez, G.; Terres, E.; Solorza, J.; Romero, S.; Yee-Madeira, H.; Flores, A.; Mora, R. Isolation and characterization of cellulose obtained from Agave salmiana fibers using two acid-alkali extraction methods. *Rev. Mex. Cienc. Agrícolas* **2016**, *7*, 31–43.

61. Bernardino, C.A.R.; Mahler, C.F.; Veloso, M.C.C.; Romeiro, G.A. Preparation of Biochar from Sugarcane By-product Filter Mud by Slow Pyrolysis and Its Use Like Adsorbent. *Waste Biomass-Valorization* **2017**, *8*, 2511–2521. [CrossRef]

62. Xiao, X.; Chen, B.; Chen, Z.; Zhu, L.; Schnoor, J.L. Insight into Multiple and Multilevel Structures of Biochars and Their Potential Environmental Applications: A Critical Review. *Environ. Sci. Technol.* **2018**, *52*, 5027–5047. [CrossRef] [PubMed]

63. Liu, L.; Shang, D.; Zhao, Y.; Zhao, Q.; Guo, Y.; Zhang, F.; Kong, Q.; Zhang, H.; Wang, Q.; Zhao, C. Preparation of Chladophora-Based Biochar and Its Adsorption Properties for Antibiotics. *ChemistrySelect* **2024**, *9*, e202303598. [CrossRef]

64. Nama, M.; Satasiya, G.; Sahoo, T.P.; Moradeeya, P.G.; Sadukha, S.; Singhal, K.; Saravaia, H.T.; Dineshkumar, R.; Kumar, M.A. Thermo-chemical behaviour of Dunaliella salina biomass and valorising their biochar for naphthalene removal from aqueous rural environment. *Chemosphere* **2024**, *353*, 141639. [CrossRef]

65. Mondal, S.; Bobde, K.; Aikat, K.; Halder, G. Biosorptive uptake of ibuprofen by steam activated biochar derived from mung bean husk: Equilibrium, kinetics, thermodynamics, modeling and eco-toxicological studies. *J. Environ. Manag.* **2016**, *182*, 581–594. [CrossRef]

66. Show, S.; Mukherjee, S.; Devi, M.S.; Karmakar, B.; Halder, G. Linear and non-linear analysis of Ibuprofen riddance efficacy by *Terminalia catappa* active biochar: Equilibrium, kinetics, safe disposal, reusability and cost estimation. *Process. Saf. Environ. Prot.* **2021**, *147*, 942–964. [CrossRef]

67. Chakraborty, P.; Show, S.; Banerjee, S.; Halder, G. Mechanistic insight into sorptive elimination of ibuprofen employing bi-directional activated biochar from sugarcane bagasse: Performance evaluation and cost estimation. *J. Environ. Chem. Eng.* **2018**, *6*, 5287–5300. [CrossRef]

68. Zhan, D.; Ye, A.; Hou, T. Research progress on biochar-based material adsorption and removal of ibuprofen. *Front. Environ. Sci.* **2023**, *11*, 1327000. [CrossRef]

69. Lekene, R.B.N.; Ntep, T.M.M.; Fetzer, M.N.A.; Strothmann, T.; Nsami, J.N.; Janiak, C. The efficient removal of ibuprofen, caffeine, and bisphenol A using engineered egusi seed shells biochar: Adsorption kinetics, equilibrium, thermodynamics, and mechanism. *Environ. Sci. Pollut. Res.* **2023**, *30*, 100095–100113. [CrossRef]

70. Osman, A.I.; Ayati, A.; Farghali, M.; Krivoshapkin, P.; Tanhaei, B.; Karimi-Maleh, H.; Krivoshapkina, E.; Taheri, P.; Tracey, C.; Al-Fatesh, A.; et al. Advanced adsorbents for ibuprofen removal from aquatic environments: A review. *Environ. Chem. Lett.* **2024**, *22*, 373–418. [CrossRef]

71. Anastopoulos, I.; Giannakoudakis, D.A.; Fronstistis, Z.; Zorpas, A.A.; Pashalidis, I.; Triantafyllidis, K. Biomass-derived adsorbents: Universal database development for their synthesis and remediation efficiency as a necessary step to move from laboratory- to pilot-scale applications. *Curr. Opin. Green Sustain. Chem.* **2024**, *47*, 100902. [CrossRef]

72. Gworek, B.; Kijeńska, M.; Wrzosek, J.; Graniewska, M. Pharmaceuticals in the Soil and Plant Environment: A Review. *Water Air Soil Pollut.* **2021**, *232*, 145. [CrossRef]

73. FAO; UNEP. *Global Assessment of Soil Pollution—Summary for Policy Makers*; FAO: Rome, Italy, 2021.

74. De Oliveira Souza, H.; dos Santos Costa, R.; Quadra, G.R.; dos Santos Fernandez, M.A. Pharmaceutical pollution and sustainable development goals: Going the right way? *Sustain. Chem. Pharm.* **2021**, *21*, 100428. [CrossRef]